Oncology and Translational Medicine
DOI 10.1007/s10330-020-0465-5

June 2021, Vol. 7, No. 3, P141–P147

ORIGINAL ARTICLE

Antitumor and vascular effects of apatinib combined with chemotherapy in mice with non-small-cell lung cancer

Hui Cao[1] (✉), Shili Wang[1], Yaohui Liu[2]

[1] Department of Pharmacy, Zigong Fourth People's Hospital, Zigong 643000, China
[2] Department of Pharmacy, Zigong First People's Hospital, Zigong 643000, China

Abstract

Objective The aim of this study was to investigate the antitumor and vascular effects of apatinib use combined with chemotherapy on mice with non-small-cell lung cancer (NSCLC).

Methods First, 60 tumor-bearing nude mice were randomly divided into control, low-dose, and high-dose groups. Four nude mice per group were sacrificed before administration and on days 1, 3, 7, and 10 after administration. HIF-1α expression in tumor tissues was detected. Second, 32 nude mice were randomly divided into control, premetrexed, synchronous, and sequential groups. The weights and tumor volumes of mice were recorded.

Results (1) HIF-1α expression decreased significantly on days 3 and 7 after low-dose apatinib treatment. There was no significant difference in HIF-1α expression in the high-dose apatinib group ($P > 0.05$). MMP-2 and MMP-9 expression levels in the low-dose apatinib group were significantly lower than those in the control group ($P < 0.05$). (2) In the low-dose apatinib group, the microvessel density increased gradually from days 3 to 7 post-treatment, while that in the high-dose apatinib group decreased significantly. (3) The inhibitory effect of sequential therapy using low-dose apatinib and pemetrexed was optimal, while that of synchronous treatment was not better than that of pemetrexed usage alone. Sequential treatment using low-dose apatinib and pemetrexed exerted the best antitumor effect. (4) The expression levels of p-AKT, p-mTOR, p-MEK, and p-ERK in the sequential group were significantly lower than those in the other three groups ($P < 0.05$).

Conclusion Apatinib usage involves certain considerations, such as dose requirements and time window for vascular normalization during lung cancer treatment in nude mice, suggesting that dynamic contrast-enhanced magnetic resonance imaging and other tests can be conducted to determine the vascular normalization window in patients with lung cancer and to achieve the optimal anti-vascular effect.

Key words: non-small-cell lung cancer (NSCLC); apatinib; pemetrexed

Received: 4 November 2020
Revised: 25 November 2020
Accepted: 20 December 2020

Lung cancer is the leading cause of cancer-related deaths worldwide, with nearly 1.2 million individuals succumbing to lung cancer every year [1]. Non-small-cell lung cancer (NSCLC) accounts for more than 80% of the lung cancer cases. Although chemotherapy can improve the outcome and quality of life of patients to some extent, the prognosis remains poor, and the median survival time is often less than 10 months [2]. Tumor growth depends on tumor angiogenesis; hence, anti-angiogenesis strategies play an important role in tumor treatment [3]. The traditional view is that antiangiogenic drugs can reduce tumor blood vessel formation, leading to tumor necrosis and "starvation" of the tumor. Short-term use of antiangiogenic drugs can be a good therapeutic strategy [4], while long-term use may lead to development of necrosis of blood vessels in the central area of the tumor, resulting in hypoxia. According to the theory of tumor angiogenesis normalization proposed by Jain *et al* [5], tumor angiogenesis is a complex process, and the imbalance between pro-angiogenic factors and angiogenesis inhibitors is a key factor. Apatinib, a small-molecule tyrosine kinase inhibitor, selectively inhibits the phosphorylation between vascular endothelial growth factor receptor 2 (VEGFR-2) and tyrosine

✉ Correspondence to: Hui Cao. Email: benbenda3321@163.com

through competitive binding with the tyrosine residue of the ATP binding site in VEGFR-2 on cells [6]. Kinase activity blocks the transmission of the VEGF/VEGFR-2 signaling pathway and inhibits tumor angiogenesis, thus inhibiting tumor growth [7]. PI3K-AKT-mTOR is one of the three major signaling pathways that have been identified to play crucial roles in cancer progression. mTOR is a key kinase downstream of PI3K/AKT, which regulates tumor cell proliferation, growth, survival, and angiogenesis. Cancer cells evade normal biochemical systems that regulate the balance between apoptosis and survival. PI3K-AKT-mTOR generally acts to promote survival through inhibition of expression of pro-apoptotic factors and activation of expression of anti-apoptotic factors. Cells contain PTEN phosphatase, which is used to negatively regulate PI3K expression. A reduction in PTEN expression indirectly stimulates PI3K-AKT-mTOR activity, thereby contributing to oncogenesis in humans. A series of clinical trials conducted on advanced lung cancer have preliminarily confirmed that apatinib can effectively decelerate lung cancer growth. However, the specific mechanism of its effect on tumor angiogenesis remains unclear.

Materials and methods

Cell lines

Human lung cancer cell line A549 was purchased from the cell bank of Chinese Academy of Sciences (Shanghai, China). A549 cells were cultured in the RPMI-1640 medium (Hyclone, Logan, USA) containing 10% fetal bovine serum, 100 U/mL penicillin, 50 mg/mL streptomycin, and 2 mmol/L glutamine; further, they were passaged and incubated in a 37°C incubator.

Establishment of xenograft tumor model in mice

Specific pathogen-free male BALB/C nude mice, aged 4–5 weeks, were purchased from the Biomedical Research Institute of Nanjing University (Nanjing, China). Approximately 2×10^6 A549 cells were suspended in 0.2 mL phosphate-buffered saline and injected subcutaneously into the right chest wall of each nude mouse. Tumor formation was observed within 10 days of injection. There was no significant difference observed in the average volumes of transplanted tumors in nude mice before intervention. In the first experiment, 60 tumor-bearing nude mice were randomly divided into three groups (20 mice per group); in the control group, normal saline was provided orally for 10 days once a day; in the low-dose apatinib group, intragastric administration of 60 mg/kg apatinib once a day, for 10 continuous days, was performed; in the high-dose apatinib group, intragastric administration of 120 mg/kg apatinib once a day, for 10 continuous days, was performed. Four nude mice per group were sacrificed before administration and on the 1st, 3rd, 7th, and 10th day after administration. In the second experiment, 32 tumor-bearing nude mice were randomly divided into 4 groups (8 mice per group); in the control group,mice were injected with normal saline of 0.5 mL.; in the pemetrexed group, intraperitoneal injection of pemetrexed 150 mg/kg was performed; in the apatinib and pemetrexed synchronous group, continuous oral administration of apatinib 60 mg/kg for 14 days along with intraperitoneal injection of pemetrexed on the first day at the same dose was performed; in the apatinib followed by pemetrexed group, first, vascular normalization was induced using apatinib for a certain period, and then pemetrexed was intraperitoneally injected during the vascular normalization window. The same abovementioned dose (60 mg/kg) was used. The time of vascular normalization was determined according to the results obtained in the first stage. Nude mice were treated for 14 days. The body weights and tumor volumes were recorded by the same person every 3 days.

Western blotting

Sonolysis of the tumor tissue was performed using a mild fluorophenyl buffer solution. A bicinchoninic acid protein detection kit was used to determine the total protein concentration. The equivalent protein amount was transferred onto a polyvinylidene fluoride membrane after subjecting the proteins to 10% sodium dodecyl sulfate polyacrylamide gel electrophoresis (SDS-PAGE). The membrane was incubated overnight with anti-mTOR, anti-p-mtor, anti-AKT, anti-erk, anti-mrk, anti-p-erk, and anti-p-mrk (diluted at 1:500) primary antibodies. The secondary antibody linked with horseradish peroxidase was added and the membrane was incubated for 3 h. After washing the membrane with Tris-Buffered Saline and Tween 20 buffer, blots were developed using enhanced chemiluminescence. Developed blots were imaged and the Image J software was used to analyze the images.

Immunohistochemistry

Immunohistochemical staining: The transplanted tumor tissue was fixed using 4% paraformaldehyde, dehydrated, and embedded in paraffin. Serial sections (3 mm thick) were obtained from each paraffin-embedded section; they were baked at 65°C for 1 h, and then dewaxed using xylene. The slides were dehydrated using ethanol, and the antigens were and repaired under high pressure with EDTA antigen repair solution. Peroxidase was removed using 3% H_2O_2 and samples were pre-treated using 5% bovine serum albumin for 30 min. They were incubated with anti HIF-1α primary antibody at 4°C overnight, and sections were incubated with biotin secondary antibody at room temperature

(25℃) for 20 min. The target protein was stained using diaminobenzidine, a peroxidase substrate. The staining intensity was estimated by three independent observers in five random regions per section.

Preparation of sample for electron microscopy analysis

The transplanted tumor tissues of mice were fixed using 3% glutaraldehyde at 4°C for 4 h, washed using 0.1 M sodium dicarboxylate buffer, and then soaked in 1% citric acid for 2 h. Then, tissues were washed twice using 0.1 M sodium dicarboxylate buffer and dehydrated using an ethanol gradient. Tissues were infiltrated with propylene oxide, completely embedded in the embedding solution, and incubated at 40°C for 12 h. The slides were then transferred to the insert plate and incubated at 60°C for 48 h. The ultrastructure of the organs was observed by transmission electron microscopy (Jeol, Japan).

Statistical analysis

All data have been expressed as mean ± standard deviation. The data were analyzed using the GraphPad prism software version 5.0. The two datasets were compared using a two-tailed unpaired Student's t-test. Multiple comparisons were performed using two-way analysis of variance and Bonferroni's post-hoc test. $P < 0.05$ was considered statistically significant.

Results

The effect of apatinib on HIF-1α expression in tumor tissues

In tumor tissues, hypoxia inducible factor (HIF) can induce an increase in angiopoietin expression, resulting in increased neovascularization, morphological variations in neovascularization, insufficiency of function, and formation of an incomplete basement membrane with uneven thickness. Therefore, HIF expression can be used as an indicator of tumor angiogenesis. The results of immunohistochemistry showed that HIF-1α expression decreased significantly on the 3rd and 7th days after treatment with lose-dose apatinib (60 mg/kg). There was no significant difference in the expression of HIF-1α in the high-dose apatinib group ($P > 0.05$; Fig. 1).

Electron microscopic observation of the ultrastructure of blood vessels

Electron microscopic observation showed that the vascular structure of the transplanted tumor was complete and exhibited regular characteristics on the 3rd and 7th days after treatment with low-dose apatinib, and the cellular structure and vascular basement membrane features were complete without formation of any gaps. When the vascular structure was disordered, a mature cell structure was not observed. At other time points and in high-dose groups, the vascular basement membrane showed incomplete formation (Fig. 2).

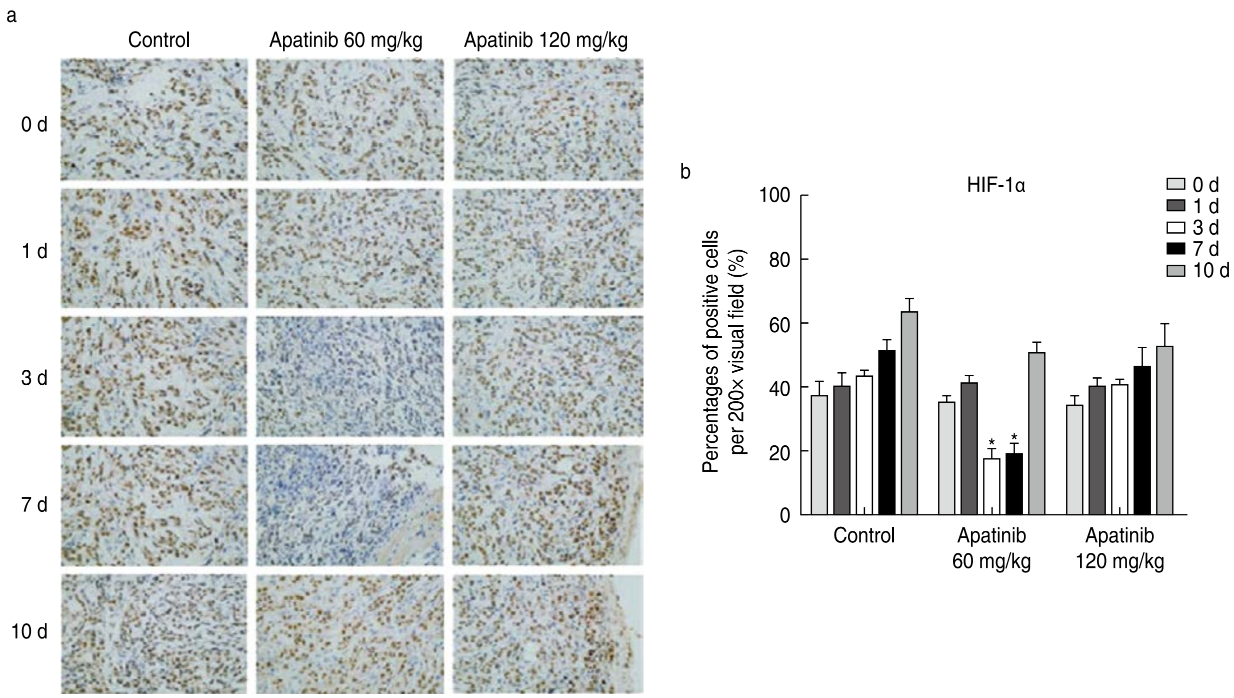

Fig. 1 Effect of apatinib on HIF-1α expression in tumor tissues. (a) Immunohistochemistry showing the expression of HIF-1α in tumor tissues; (b) Percentage of HIF-1 α expression positive cells

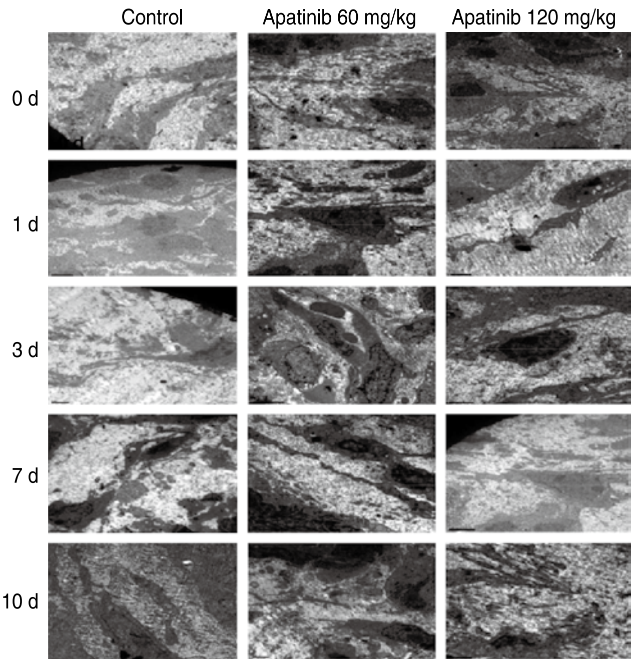

Fig. 2 Electron microscopic observation of the vascular tissue ultrastructure

Expression of MMP-2 and MMP-9 in transplanted tumor tissues

Western blotting results showed that compared with other groups, the low-dose apatinib group exhibited significantly decreased expression levels of MMP-2 and MMP-9 during days 3–7 ($P < 0.05$). MMP-2 and MMP-9 expression levels demonstrated no significant changes at other time points or in the high-dose apatinib group ($P > 0.05$; Fig. 3).

The effect of apatinib on microvessel density (MVD) in transplanted tumor tissues

MVD was detected via immunohistochemistry. The results showed that the MVD in the low-dose apatinib group increased gradually from days 3 to 7 post-treatment, and there was no significant difference during other time periods ($P > 0.05$; Fig. 4). The MVD of the high-dose apatinib group decreased significantly. This finding provides an explanation for the observation of low-dose apatinib-mediated induction of vascular normalization, while high-dose apatinib significantly destroyed the vascular structure of the transplanted tumor tissue, resulting in a significant reduction in blood vessels in the tumor tissue; thus, no time window exists for vascular normalization.

Inhibitory effect of apatinib in combination with chemotherapy on transplanted tumors

The inhibitory effect of sequential therapy with low-dose apatinib and pemetrexed was optimal, while that of synchronous treatment was not better than that of pemetrexed alone. According to the tumor inhibition curve, compared with the growth of the control group, that of the other three groups was significantly inhibited. The tumor volumes significantly differed, and the sequential treatment group had the best inhibitory effect, which was significantly different from that of

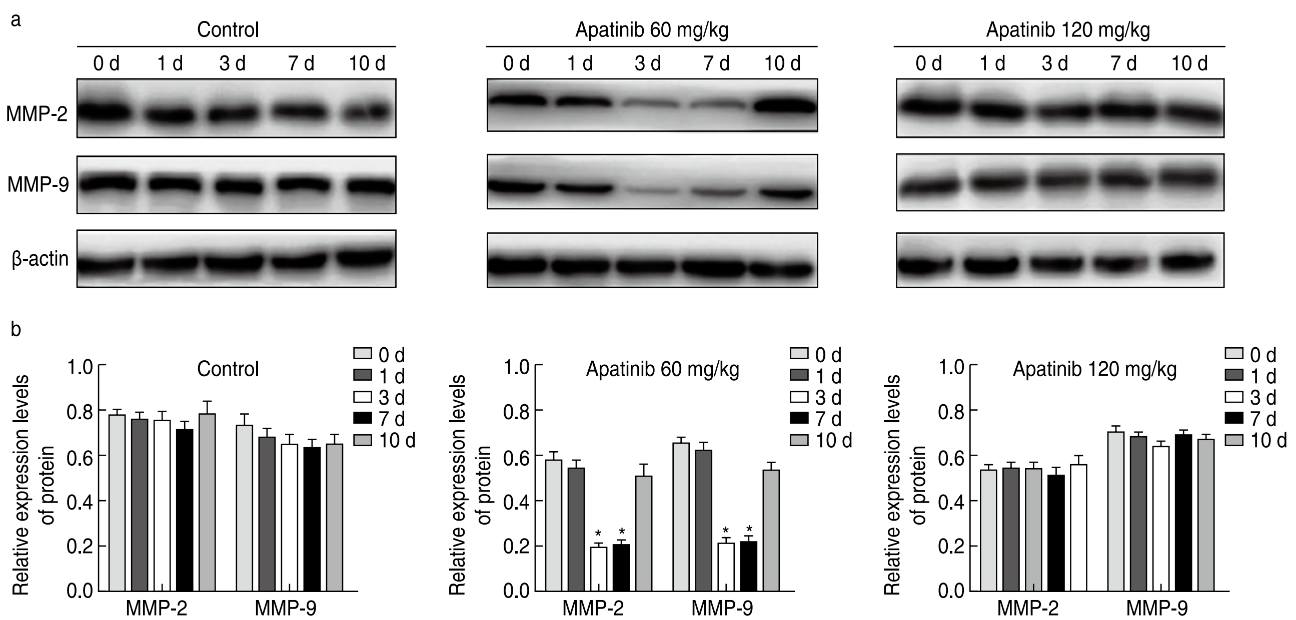

Fig. 3 MMP-2 and MMP-9 expression in transplanted tumor tissues. (a) Western blot analysis of the expression of MMP-2 and MMP-9 in transplanted tumor tissue; (b) Relative expression of MMP-2 and MMP-9 in transplanted tumor tissues

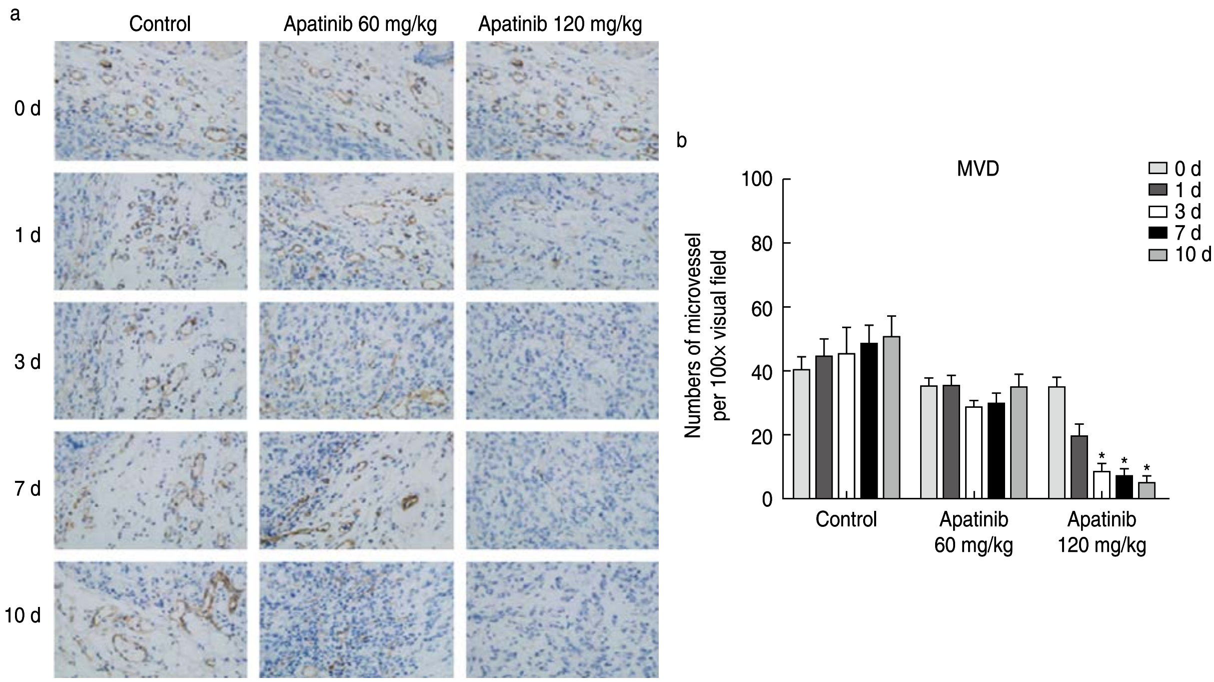

Fig. 4 Effect of apatinib on MVD in transplanted tumor tissues. (a) Immunohistochemical detection of the effect of apatinib on microvessel density in transplanted tumor tissues; (b)The number of microvessels in the transplanted tumor tissues

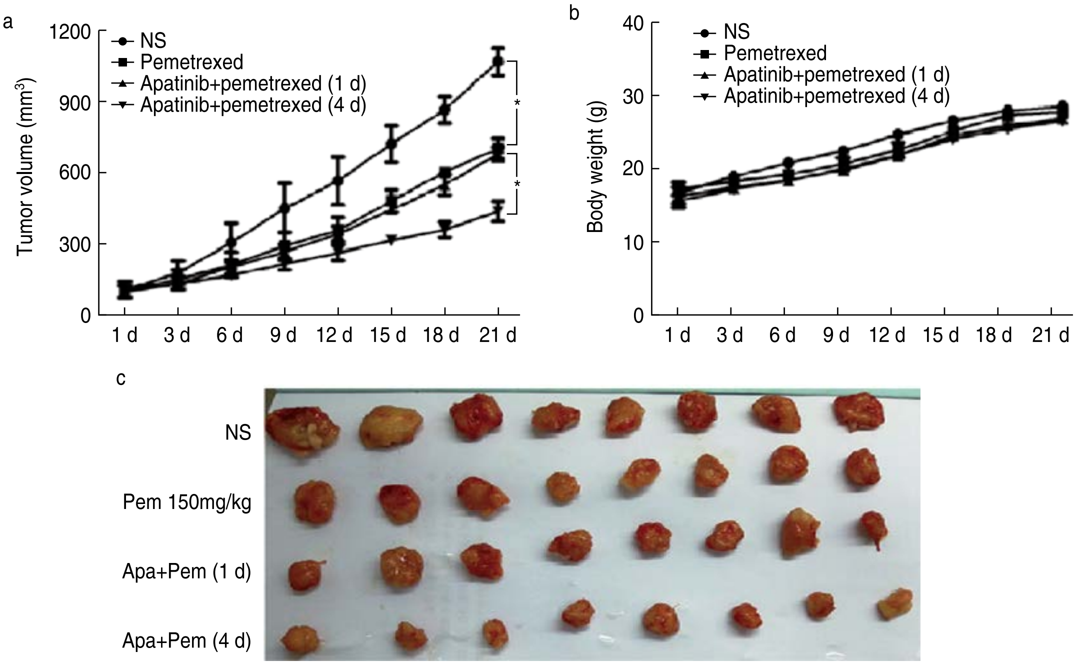

Fig. 5 Inhibitory effect of apatinib combined with chemotherapy on transplanted tumors. (a) Effect of apatinib combined with chemotherapy on the volume of transplanted tumors; (b) Effect of apatinib combined with chemotherapy on the weight of transplanted tumors; (c) Inhibitory effect of apatinib in combination withchemotherapy on transplanted tumors

synchronous treatment ($P < 0.05$; Fig. 5).

Expression of related signaling pathway factors in transplanted tumor tissue

The PI3K-AKT-mTOR signaling pathway plays an important role in cancer stem cell self-renewal and development of resistance to chemotherapy or

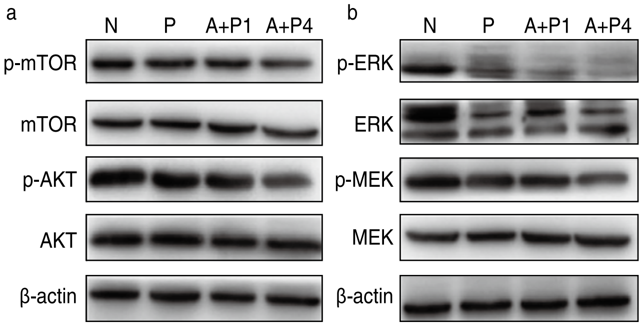

Fig. 6 Effect of apatinib on protein expression of related signaling pathways. (a) Western blot analysis of the effect of apatinib on the expression of PI3k-Akt-mTOR pathway protein; (b) Western blot analysis of the effect of apatinib on the expression of MEK-ERk-MNk pathway protein

radiotherapy, which has been suggested to be attributable for treatment failure, cancer recurrence, and metastasis. The expression levels of p-AKT, p-mTOR, p-MEK, and p-ERK in the sequential group were significantly lower than those in the other three groups ($P < 0.05$; Fig. 6). This suggests that sequential therapy using low-dose apatinib and pemetrexed may exert biological effects through the above-mentioned signaling pathways and may inhibit the growth of xenografts.

Discussion

Since the first antiangiogenic drug bevacizumab was administered for clinical use, antiangiogenic therapy has become an important strategy to treat malignant tumors. Particularly, the application of small-molecule antiangiogenic drugs via oral administration to cancer patients has demonstrated appreciable effects. Apatinib is a specific VEGFR-2 receptor antagonist, which competitively binds to VEGFR-2 receptors, blocks the VEGF-mediated signaling pathway, inhibits tumor angiogenesis, and thus controls tumor growth [8]. Presently, more than 30 clinical studies have examined the treatment of advanced lung cancer with apatinib. Most patients present with progressive NSCLC, while a few present with small-cell lung cancer. Most treatments focus on third-line therapy as the suitable approach. Apatinib monotherapy also includes apatinib use combined with chemotherapy or targeted drug therapy. In all clinical studies, monotherapy demonstrated poor efficacy [9]. The median progression-free survival (PFS) was less than 3 months, and the disease control rate was less than 50%. Therefore, the National Comprehensive Cancer Network guideline no longer recommends utilization of apatinib monotherapy for lung cancer [10]. According to the efficacy of apatinib usage combined with chemotherapy reported in the treatment of advanced lung cancer, compared with apatinib usage alone, the combination therapy can improve the PFS and overall survival (OS) of patients to a certain extent, but the OS time remains short.

Traditionally, antiangiogenic drugs inhibit blood flow mainly by inhibiting blood vessel formation in tumors, resulting in tumor "starvation." Antiangiogenic drugs can effectively control tumor growth for a certain period, but tolerance to therapy and tumor recurrence occurs inevitably [11]. At this juncture, combination therapy may be an effective strategy, including combined chemotherapy, targeted therapy, or immunotherapy. However, the clinical results of apatinib usage combined with chemotherapy for the treatment of advanced lung cancer did not significantly improve PFS and OS, which might be related to the mode of administration. Conventional doses of antiangiogenic drugs can effectively reduce tumor angiogenesis. During the administration of combined chemotherapy drugs, due to the rapid reduction in tumor neovascularization, especially in the tumor center, the effective concentration of local chemotherapy drugs is observed to be lower than expected, which markedly affects the tumor sensitivity to these drugs. Additionally, ischemia, hypoxia, and acidosis further affect the metabolism and transportation of drugs, resulting in exertion of poor treatment effects [12]. Astrid *et al.* [13] found that bevacizumab reduced docetaxel administration flow and net flow within 5 h in NSCLC patients, and these effects lasted for a period of 4 days. This further indicates that antiangiogenic drugs can easily induce local chemotherapy drug transport and reduce the effective blood concentration of the drug.

Based on these results, the combination of antiangiogenic drugs and chemotherapy drugs is not recommended. Since Jain first proposed the "vascular normalization theory" in 2005, accumulating studies have supported this perspective. After treatment with anti-vascular drugs, tumor blood vessels exhibit "normalized" characteristics within a certain period; that is, tumor blood vessels and cell morphology exhibit normal features, and the integrity of the basement membrane structure is partially restored, to improve hypoxia and acidosis in the tumor [14]. This state reduces the interstitial pressure in the tumor tissue, thus improving the transport, local effective concentration, and efficacy of chemotherapy drugs in the tumor. Our findings further confirm this phenomenon. Tumor tissues release various factors that promote growth of new blood vessels. Under the effect of VEGF, the most crucial angiogenic factor, tumor blood vessels grow rapidly, and vascular distortion, disorder, local expansion, leakage, and increased interstitial pressure occur. Increased pressure can lead to development of ischemia and hypoxia, and increased HIF expression, resulting in the establishment of a series of biological effects. Apatinib is the most specific VEGFR-2 inhibitor, which can effectively reduce the effect of VEGF [15]. In this experiment, we observed that HIF-1α expression in the transplanted tumor tissue decreased significantly after 3–7 days of low-dose apatinib administration. These results indicate that after the intervention using low-dose apatinib, the local hypoxic state of the transplanted tumor tissue was significantly improved, and the tumor vascular structure was relatively complete, thus realizing transient normalization. In the high-dose apatinib group, we did not observe a clear window of vascular normalization. Immunohistochemistry results also showed that MVD was significantly decreased in the high-dose apatinib group, especially in the center of the transplanted tumor. The MVD decreased and there was no neovascularization, indicating that MVD did not return to normalcy. Therefore, we believe that the appearance of the vascular normalization window is related to the timing of antiangiogenic drug administration as well as the dose [16]. To further confirm that the window of vascular normalization during treatment with antiangiogenic drugs in combination with chemotherapy could effectively improve the therapeutic effect of chemotherapeutic drugs, we constructed a nude mouse model using transplanted tumors. The results showed that pemetrexed chemotherapy on day 4 following low-dose apatinib administration could significantly reduce the transplanted tumor volume. Therefore, sequential therapy with low-dose apatinib and pemetrexed can effectively inhibit the proliferation and promote the apoptosis of the transplanted tumor. Moreover, the PI3k-AKT-mTOR and the MEK-ERk-MNk signaling pathways play biological roles in these outcomes. It is suggested that the window of tumor vessel normalization is not observed immediately after application of an appropriate dose of antiangiogenic drugs, and the addition of chemotherapeutic drugs during this window can effectively improve their efficacy.

In conclusion, this study reports that there a certain dose is required for apatinib use and there exists a time window for vascular normalization in the treatment of lung cancer in nude mice, which suggests that DCE-MRI and other tests can be conducted to determine the vascular normalization window in patients. Furthermore, we should also follow the principle of individualized administration to enable treatment of each patient within the appropriate window of vascular normalization.

Conflicts of interest

The authors indicated no potential conflicts of interest.

References

1. Roman M, Baraibar I, Lopez I, *et al*. KRAS oncogene in non-small cell lung cancer: clinical perspectives on the treatment of an old target. Mol Cancer, 2018, 17: 1–14.
2. Wei X, Shen X, Ren Y, *et al*. The roles of microRNAs in regulating chemotherapy resistance of non-small cell lung cancer. Current Pharm Design, 2017, 23: 5983–5988.
3. Wilner KD, Usari T, Polli A, *et al*. Comparison of cardiovascular effects of crizotinib and chemotherapy in ALK-positive advanced non-small-cell lung cancer. Future Oncol, 2019, 15: 1097–1103.
4. Bacic I, Karlo R, Zadro A S, *et al*. Tumor angiogenesis as an important prognostic factor in advanced non-small cell lung cancer (Stage IIIA). Oncol Lett, 2017, 15: 2335–2339.
5. Jain R K. Antiangiogenic therapy for cancer: current and emerging concepts. Oncology, 2005, 19: 7–15.
6. Liu S, Su L, Mu X, *et al*. Apatinib inhibits macrophage-mediated epithelial–mesenchymal transition in lung cancer. RSC Advances, 2018, 8: 21451–21459.
7. Zhang H, Cao Y, Chen Y, *et al*. Apatinib promotes apoptosis of the SMMC-7721 hepatocellular carcinoma cell line via the PI3K/Akt pathway. Oncol Lett, 2018, 15: 5739–5743.
8. Liu M, Wang X, Li H, *et al*. The effect of apatinib combined with chemotherapy or targeted therapy on non-small cell lung cancer in vitro and vivo. Thorac Cancer, 2019, 10: 1868–1878.
9. Huang M, Gong Y, Zhu J, *et al*. A phase I dose-reduction study of apatinib combined with pemetrexed and carboplatin in untreated EGFR and ALK negative stage IV non-squamous NSCLC. Invest New Drugs, 2020, 38: 478–484.
10. Lan C Y, Wang Y, Xiong Y, *et al*. Apatinib combined with oral etoposide in patients with platinum-resistant or platinum-refractory ovarian cancer (AEROC): a phase 2, single-arm, prospective study. Lancet Oncol, 2018, 19: 1239–1246.
11. Nagano T, Tachihara M, Nishimura Y. Molecular mechanisms and targeted therapies including immunotherapy for non-small cell lung cancer. Curr Cancer Drug Targets, 2019, 19: 595–630.
12. Liu Z, Ou W, Li N, *et al*. Apatinib monotherapy for advanced non-small cell lung cancer after the failure of chemotherapy or other targeted therapy. Thorac Cancer, 2018, 9: 1285–1290.
13. Van der Veldt AA, Lubberink M, Bahce I, *et al*. Rapid decrease in delivery of chemotherapy to tumors after anti-VEGF therapy: implications for scheduling of anti-angiogenic drugs. Cancer Cell, 2012, 21: 82–91.
14. Wang J, Ma S, Chen X, *et al*. The novel PI3K inhibitor S1 synergizes with sorafenib in non-small cell lung cancer cells involving the Akt-S6 signaling. Invest New Drugs, 2019, 37: 828–836.
15. Nielsen S H, Willumsen N, Brix S, *et al*. Tumstatin, a matrikine derived from collagen type IVα3, is elevated in serum from patients with non–small cell lung cancer. Transl Oncol, 2018, 11: 528–534.
16. Chen Y, Mathy NW, Lu H. The role of VEGF in the diagnosis and treatment of malignant pleural effusion in patients with non-small cell lung cancer (Review). Mol Med Rep, 2018, 17: 8019–8030.

DOI 10.1007/s10330-020-0465-5

Cite this article as: Cao H, Wang SL, Liu YH. Antitumor and vascular effects of apatinib combined with chemotherapy in mice with non-small-cell lung cancer. Oncol Transl Med, 2021, 7: 141–147.